Spectral Intensity and Charge Distributions in the Tetrahedral Chromophores, Bis(3-amino-2-methylpropane-2-thiolato)- and Diacetatobis(ethylenethiourea)-cobalt(II)

Melinda J. Duer and Malcolm Gerloch*
University Chemical Laboratory, Lensfield Road, Cambridge CB2 1EW

Ligand-field analyses of both transition energies and relative intensities are reported for the spin-allowed '*d*–*d*' bands of bis(3-amino-2-methylpropane-2-thiolato) cobalt(II). Energy $\{e_\lambda\}$ and transition moment $\{{}^{L}t_\lambda\}$ parameter values that reproduce experiment are critically compared with each other and with similar quantities from an earlier analysis of diacetatobis(ethylenethiourea) cobalt(II). The nature of the parameterization scheme in the intensity model is described and the chemical significance of its variables is reviewed and developed. The thiolate ligands in the first chromophore are revealed as strong σ donors but essentially π innocent. The thiourea ligators in the second chromophore are only weak bases but the acetates are shown to be both good σ and π donors. It is argued that the electron distribution in these cobalt–oxygen bonds is relatively well polarized towards the metal and contracted about the internuclear axis. These latter conclusions arise from an analysis of the spectral intensities.

Traditional ligand-field analysis has been concerned almost exclusively with '*d*–*d*' transition energies and magnetic properties.[1–5] The most powerful and chemically transparent models of the ligand field employ the principle of spatial superposition. The Cellular Ligand Field (c.l.f.) approach[4] is characterized by parameters like e_σ and e_π which provide discrimination not only between contributions from different ligands but also between bonding modes. These parameters, like Δ_{oct}, relate to '*d*' orbital *energies*. On the other hand, the orbital reduction factor k in the magnetic moment operators $\mu_\alpha = kl_\alpha + 2s_\alpha$ where $\alpha = x$, y, or z, used in computations of consequential magnetic properties, effectively parameterize the ligand-field *wave-functions*.

Very recently, we have introduced a new approach[6–8] for the computation of the *intensities* of ligand-field spectra. As for the rest of ligand-field analysis, it is parametric. Electric dipole transition moments of the kind $\langle$'*d*'$|er|$'*d*'$\rangle$ are expressed in terms of a set of t parameters which, like the orbital reduction factor above, relate to the imperfect purity of the ligand-field d orbitals. While the formalism and structure of the new model need not be repeated here, it is appropriate to review the parameterization scheme, at least briefly, for therein lies the chemical and bonding relevance we require.

The d electrons of ligand-field theory are only imperfectly decoupled from the bonding framework in a complex. Let us express the impurity of the ligand-field '*d*' orbitals by equation (1) where χ describes all non-d functions that are admixed by

$$\text{'}d\text{'} \approx d + b\chi \qquad (1)$$

any static† means. Correlations with chemistry are ultimately made by arguing that χ is dominated by the bond orbitals in the complex; χ may be expanded, with no loss of generality, as a sum of multipoles with $s, p, d, f, \cdots$ character [equation (2) in which

$$\chi_\lambda = a_1 s_\lambda + a_2 p_\lambda + a_3 d_\lambda + a_4 f_\lambda + \cdots \qquad (2)$$

λ labels symmetry]. All parts of equation (2) implicitly contribute to the orbital reduction factor, k, in magnetic moment operators. On the other hand, the selection rule $\Delta l = \pm 1$ selects only those multipoles of p or f character as relevant for a computation of electric dipole transition moments. Our model separates intensity contributions arising from these two characters. The only surviving parts of a transition moment $\langle$'*d*'$|er|$'*d*'$\rangle$ are then of the forms $\langle d|er|p\rangle$, $\langle d|er|f\rangle$, and $\langle\chi|er|\chi\rangle$, together with appropriate multipliers deriving from the expansion (2) and the original ligand-field orbital (1). Those multipliers and, indeed, the detailed radial forms of any of the functions appearing in these integrals are unknown to us in any particular system. As elsewhere in ligand-field analysis, we content ourselves with their partition and parameterization.

The parameterization scheme exploits the advantages of spatial superposition as for the c.l.f. modelling of ligand-field energies. There, we refer to e_σ and e_π energy parameters for local $C_{\infty v}$ pseudo-symmetry or to e_σ, $e_{\pi x}$, and $e_{\pi y}$ for C_{2v}. The intensity model is similarly structured but, in addition to a partitioning that separates ligand and bonding modes, there arises a further division, defined as follows. Parameters are labelled ${}^{L}t_\lambda$ where $L = P$, F, or R and $\lambda = \sigma, \pi_x$, or π_y [equation (3)—(5)] where z

$${}^{P}t_\lambda = b_p^\lambda \langle d_\lambda|ez|p_\lambda\rangle \qquad (3)$$

$${}^{F}t_\lambda = b_f^\lambda \langle d_\lambda|ez|f_\lambda\rangle \qquad (4)$$

$${}^{R}t_\lambda = b_\lambda^2 \langle \chi_\lambda|ez|\chi_\lambda\rangle \qquad (5)$$

is the component of the light vector parallel to the M–L axis, and the $\{b_p\}$ and $\{b_f\}$ subsume the $\{b\}$ of equation (1) and the appropriate $\{a\}$ coefficients of (2). While the partitioning of variables by symmetry and the label λ surely need no further comment, the superscripts P, F, and R bring an increased degree of parameterization that requires discussion.

First, for every one e_λ parameter required in a ligand-field energy analysis, the reproduction of intensities requires three ${}^{L}t_\lambda$. Nevertheless, experience to date has shown[7–9] that these intensity analyses tend to proceed more smoothly than their energy counterparts, usually yielding essentially unique optimum parameter sets. In any case, the degree of parameterization is often effectively less than at first apparent because of the special circumstances for the ${}^{R}t_\lambda$ variables. We

† Throughout this paper, we consider intensity-giving parity mixing that arises in non-centric environments. Dynamic mixing and vibronic coupling are explicitly disregarded.

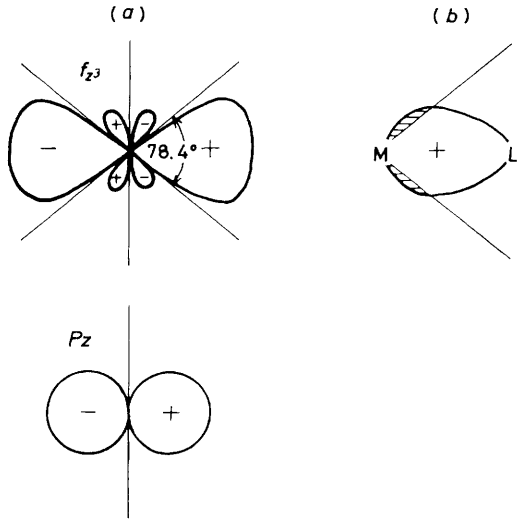

Figure 1. (*a*) Nodal cone angles of f_σ and p_σ functions. (*b*) That part of a bond orbital χ lying outside the cone of the f_σ must be represented by multipoles with lower l values. The more polarized χ is towards the metal atom, the greater the ratio of P:F contributions to the intensity parameters

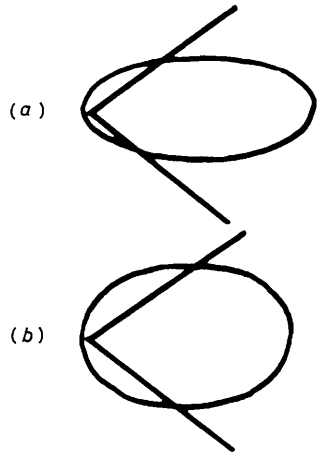

Figure 2. How relatively larger P contributions are associated with 'fatter' bond orbitals (*b*) than 'thinner' ones (*a*)

have shown[8] that contributions from these parameters cancel throughout a chromophore with bipyramidal or antiprismatic geometry. In practice, such contributions are small and virtually indeterminate also for systems whose ligand fields approach these geometric ideals. We are left, therefore, with just two sets of ${}^{L}t_{\lambda}$ where $L = P$ or F for each ligand type, rather than three. For the present purposes, therefore, we focus on the significance of this 'double layer' of intensity parameterization.

We consider the likely response of the magnitudes of these parameters and their ratios with variation of bond length, choice of metal and ligand, and bond polarization. We confine attention in this Introduction to the case of σ bonding as this is most relevant to the actual systems investigated in the present study. One approach is by reference to the multipolar expansion (2). No essential loss of generality accompanies the form of expansion chosen in (2) in which the non-*d* admixture is expressed as a sum of only *one s* multipole, *one p*, *one f*, *etc.* The expansion is implemented by variation not only of the coefficients $\{a\}$ in (2) but also of the radial forms of the expansion coefficients themselves. So reproduction of a more extended χ function, as would accompany longer metal–ligand bonds, for instance, would involve more diffuse functions as well as increased participation of the higher-order multipoles. We therefore conclude that the contribution to spectral intensities from the F type parameters of equation (4) relative to that from the P parameters of (3) will increase with increasing metal–ligand separation, or with increasing polarization of χ towards the ligand, or both. Idealized modelling computations[8] of the $\langle d|er|p,f\rangle$ integrals in these parameters have confirmed these predictions.

These arguments may also be expressed in useful pictorial terms. In Figure 1 are sketched the angular forms of p_σ and f_σ orbitals that would be part of the expansion of the non-*d* part, χ_σ, of a ligand-field orbital. It is evident that increasing polarization towards the metal, arising from either decreasing bond length or greater transfer of electron density from ligand to metal, increases those portions which lie outside the nodal cone of the f_σ functions. Those parts must be represented in the multipole expansion, therefore, by functions with wider cone angles and hence with smaller quantum number l. As we are only concerned with the p and f parts in these expansions, we observe the same result as above; namely, that shorter bonds and/or greater ligand polarization towards the metal is expected to increase the ${}^{P}t_\sigma$ parameters relative to the ${}^{F}t_\sigma$.

The relative contributions of P type and F type intensity parameters will also reflect the lateral bulk of χ functions and, by inference, of bond orbitals. It is immediately obvious from the sketches in Figure 2 that 'fatter' bonds will be associated with greater P contributions than 'thinner' ones. The same conclusion can be reached also from consideration of the multipole expansion, as above. Thus, 'fatter' ligand-field orbitals will be reproduced in that expansion with increasing, or more diffuse, radial forms of the expansion functions. In order to counteract the concomitant effects along the line of centres, greater weight must then be given to the lower-order multipoles.

While other trends in both σ and π bonding situations have been discussed elsewhere[8,9] we focus here on these two particular trends, relating to variations in electron density parallel and perpendicular to a metal–ligand vector. They are illustrated and exploited in analyses of two somewhat related chromophores. Bis(3-amino-2-methylpropane-2-thiolato)-cobalt(II) provides an asymmetrically bis chelated CoN_2S_2 chromophore of nominal tetrahedral symmetry.[10] Single-crystal polarized absorption spectra have been recorded[11] for this complex to help model the spectrum of the active site in cobalt(II) reconstituted horse liver alcohol dehydrogenase. Our concern here is entirely with the quantitative reproduction of the transition energies and relative band intensities of the '*d*–*d*' spectrum of the model compound. We compare the results of that analysis with those recently published[8] on the pseudo-tetrahedral complex, diacetatobis(ethylenethiourea)cobalt(II), with the chromophore CoO_2S_2. We are able then to comment on the interactions between cobalt(II) and acetate, amine, thiolate, and thioketone.

Analyses

Bis(3-*amino*-2-*methylpropane*-2-*thiolato*)*cobalt*(II).—The molecular structure of $[Co\{SC(CH_3)_2CH_2NH_2\}_2]$, abbreviated hereafter as CoN_2S_2, is shown in Figure 3. These tetrahedral chromophores possess crystallographic two-fold symmetry and pack in an orthorhombic lattice.[10] Polarized spectra have been recorded[11] with light incident on the (001) face with the electric vector parallel to *a* and *b*. Earlier detailed crystal spectroscopy[10] focused particularly on some spin-forbidden features. Bands assigned to spin-allowed ligand-field '*d*–*d*' transitions occur at 10 400, 15 500, 17 800, and 18 300 cm^{-1}. Using our CAMMAG2 program suite,[12] we have sought to reproduce these transition energies within the c.l.f. model. Except for final calculations, all

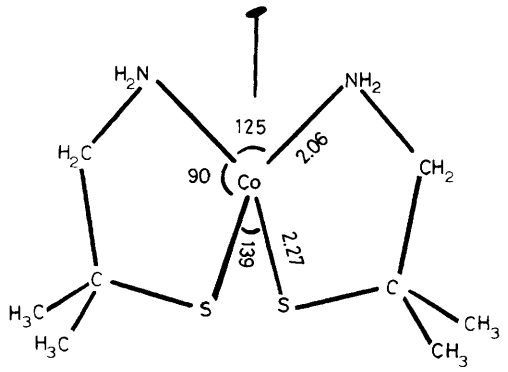

Figure 3. The co-ordination[10] in the CoN_2S_2 chromophore; distances in Å, angles in °

Table 1. Comparison between observed[11] spin-allowed transition energies (cm^{-1}) and those calculated* with the optimal parameter set in Table 3 for CoN_2S_2

Obs.	Calc.
18 300	18 398
17 800	17 794
15 500	15 406
10 400	10 342
	9 827
	7 119
	6 620
	3 315
	2 703
	0

* Calculated within full d^7 basis, using C = 2 900 cm^{-1}.

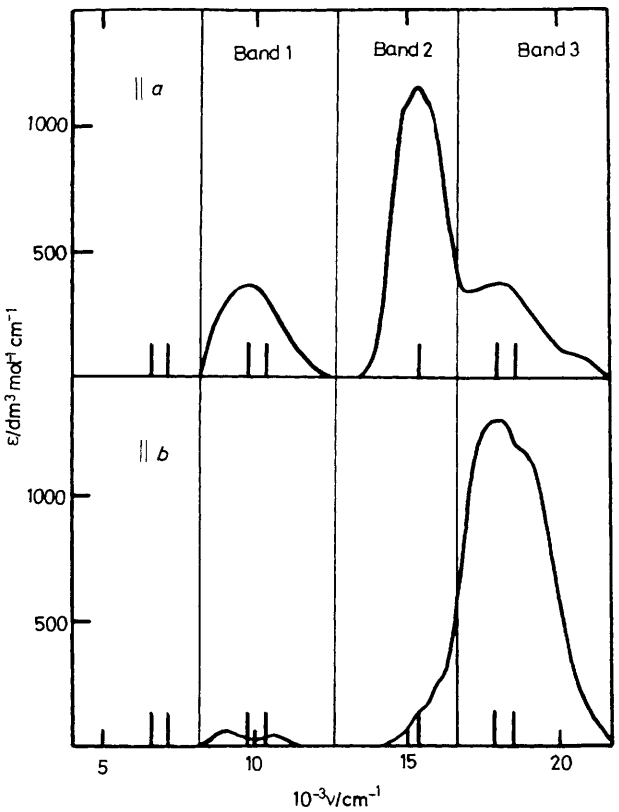

Figure 4. The polarized crystal spectra[11] at 80 K of CoN_2S_2. The bands define integration bounds for areas in the spectra. Calculated spin-quartet transition energies are indicated by the longer markers

computations were performed within the spin-quartet basis, $^4F + {}^4P$. In addition to the Racah parameter B for interelectron repulsion energies and the spin–orbit coupling coefficient ζ, fixed throughout at 500 cm^{-1}, the model is parameterized with e_σ(N) for the amine ligators, and e_σ(S) and $e_{\pi\perp}$(S) for the thiolates. The 'perpendicular' label refers to possible interaction with the nominal p orbital on each sulphur atom lying perpendicular to the appropriate Co–S–C plane; the angle Co–S–C is 95°. We thus hope to define four parameter values with four transition energies. Wide ranges were systematically considered for each parameter: e_σ(N) from 2 500 to 6 000 cm^{-1}; e_σ(S) from 2 000 to 7 000 cm^{-1}; $e_{\pi\perp}$(S) from −2 000 to +2 000 cm^{-1}; and B from 400 to 800 cm^{-1}. A smooth exploration yielded excellent reproduction of experiment with a unique set of parameter values. The quality of agreement is shown in Table 1 and the optimal parameter set in Table 3. Final calculations were carried out within the full 120-fold basis of d^7. With the Racah parameter C at 2 900 cm^{-1}, a spin doublet was calculated to lie at 8 720 cm^{-1}, in agreement with an observed feature at 9 100 cm^{-1}. No significant changes in other parameter values or in calculated spin-quartet energies were noted.

This energy analysis was followed with one of spectral intensities. For this, the spectral traces were divided into three regions: 8 000—12 500, 12 500—16 550, and 16 550—21 800 cm^{-1}. The resolution between these ranges was estimated as in previous analyses and shown in Figure 4. Integrations of all intensity in each polarization falling within these bounds were made empirically by cutting out and weighing copies of the spectra. In the first instance, we sought to reproduce these six pieces of data with the intensity model described in the Introduction and elsewhere:[6–8] computations were performed once more within the CAMMAG2 system.[12] Initially, calculations were carried out within the restricted spin-quartet

Table 2. Comparisons for CoN_2S_2 between observed[11] intensity distributions and those calculated* with the optimal parameter sets of Table 3. Sums of observed and corresponding calculated intensities are normalized to 100 (arbitrary units)

	Relative intensities			
	‖ a		‖ b	
Band interval/ 10^3 × cm^{-1}	obs.	calc.	obs.	calc.
9.0—12.0	10	14	1	0.8
12.5—17.0	24	19	2	0.2
17.0—22.0	14	17	51	49

* Calculated in d^7 spin-quartet basis.

basis, $^4F + {}^4P$, for reasons of speed and economy: final calculations employed the full d^7 configurational basis. The parameter set comprised $^{P,F}t_\sigma$(N), $^{P,F}t_\sigma$(S), and $^{P,F}t_{\pi\perp}$(S), but was extended later to include the equivalent R type variables.[6,8] At first, therefore, we sought to reproduce the six intensities with six t parameters. An essentially full coverage of parameter space was explored by setting, in turn, several parameter values to 100 (arbitrary units, but see later) followed by variation of all others between ± 100 in steps of 10. As for the energy analysis above, a smooth process yielded reasonably good reproduction of experiment with an essentially unique set of parameter values. The fit and optimal parameter set were markedly insensitive to variations in the spin–orbit coupling coefficient between 350 and 500 cm^{-1}. Extension of the basis to d^7 with the Racah parameter C again set at 2 900 cm^{-1} altered calculated intensities by less than 1%. Calculated intensities are compared

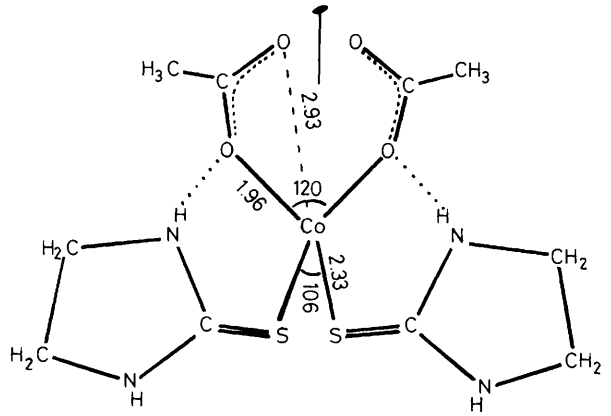

Figure 5. The co-ordination[13] in the CoO_2S_2 chromophore; distances in Å, angles in °

with experiment in Table 2 for the optimal t parameter set given in Table 3. At this point, the response of the calculations to inclusion of ${}^{R}t_{\lambda}$ parameters was investigated. Values of any R type parameter less than 40 on the same scale as Table 3 made no significant change. With larger values, only small changes were observed but we were unable to determine optimal values with any reasonable accuracy. This undoubtedly reflects the approximate (skew) antiprismatic symmetry of this chromophore. As shown elsewhere,[8] R type contributions to the intensities cancel identically in that ideal geometry.

Though not part of the fitting or refinement process, it was also of interest to compute the relative intensities of the unresolved components within the bands. With the same parameter values as above and within the full d^7 basis, we calculate intensities for the spin-allowed transitions at 17 800 and 18 300 cm^{-1} to be in the ratio *ca.* 1:2 in *a* polarization and 5:1 in *b* polarization. These ratios agree with experiment as best as we might estimate those from Figure 4. Then, for the composite band at *ca.* 15 500 cm^{-1}, calculations within the full basis yield a doublet 180 cm^{-1}, to the red of the quartet and another doublet 425 cm^{-1} further to the blue: their relative intensities in *a* polarization are calculated to be in the ratio 5:18:1, once again compatible with the observed band profile.

Di(acetato)bis(ethylenethiourea)cobalt(II).—The molecular structure[13] of this chromophore, which possesses two-fold symmetry, is shown in Figure 5. The acetates are considered as effectively unidentate and we abbreviate the system hereafter as CoO_2S_2. Both energy and intensity analyses have been reported[7,8] in full. We obtained unique fits in both cases and include the optimum parameter sets in Table 3.

Discussion

We consider the two chromophores together with regard to both energy and intensity parameters as listed in Table 3. The e_{σ} parameter values describe a greater basicity of the thiolate than the amine in CoN_2S_2 and much greater than for the thiourea in CoO_2S_2. Neither sulphur ligand shows much π bonding character so that, overall, the thioketone furnishes a very weak ligand field. We have observed earlier[14,15] the tendency for the ligand-field trace, Σ, defined as the sum of all locally diagonal e_{λ} parameters, to vary little throughout extended series of complexes for metals in the same oxidation state. The same result characterizes the two sets of energy parameters here. This constancy probably arises from the operation of the electroneutrality principle establishing closely similar net

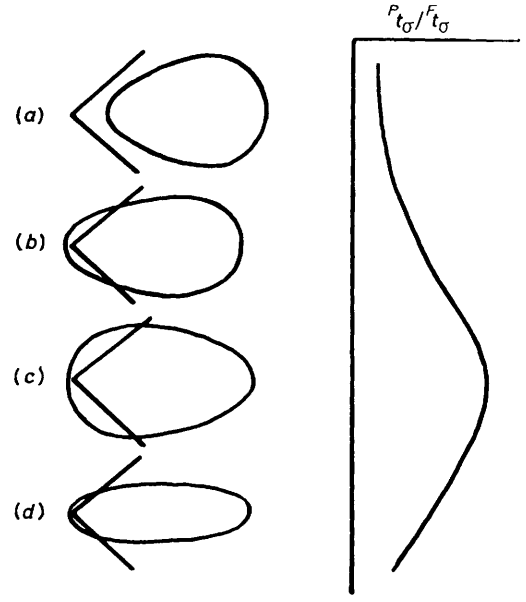

Figure 6. Schematic illustration of the way the ratio ${}^{P}t_{\sigma}/{}^{F}t_{\sigma}$ should vary with electron distribution in a metal–ligand bond. In (*a*)—(*c*) are shown bonds progressively more polarized towards the metal; in (*d*) the bond is compacted about the internuclear axis

charges of the central metal. In the CoO_2S_2 system, that charge redistribution appears to be implemented by the acetate ligands acting as both strong σ donors and strong π donors in compensation for the weak thiourea ligators. No doubt the metal draws upon the delocalized π-electron density of the acetate anions. Altogether then, while the ligand field in CoO_2S_2 is dominated by the acetate groups, it is the sulphur ligands in CoN_2S_2 that provide the larger perturbation.

Overall, the relative donor strengths of the various ligands in these two complexes correlate as well as might be expected with bond lengths. The stronger cobalt–thiolate ligations have bond lengths of 2.27 Å while the weak cobalt–thiourea distances are 2.33 Å. Both Co–O and Co–N bonds are of typical length for many tetrahedra. One may compare, however, the large e_{σ} and e_{π} values for the present Co–O bonds, at 1.96 Å, with the values[16] $e_{\sigma} = 3\,600$ and $e_{\pi} \approx 800$ cm^{-1} for the cobalt–oxygen interactions, at 2.01 Å, for arsine oxide ligations in the five-co-ordinate complex $[Co(OAsPh_2Me)_4(NO_3)]^+$.

Now consider the t parameter values independently established from the spectral intensities. As the spectra for the CoO_2S_2 chromophore were reported[13] on arbitrary (common) scales, it is not possible to compare the magnitudes of the parameters between the two systems. In each case, therefore, we follow our usual practice of reporting t parameters normalized for each chromophore such that the largest value is set at 100 arbitrary units.* We therefore comment on the relative magnitudes of the t parameters within each chromophore and compare these with the appropriate e parameter values. Throughout, we observe that large e values are associated with large t values, small with small, and even middling with middling. Similar qualitative correlations are evident in all such comprehensive ligand-field analyses completed to date and serve to encourage confidence in this new approach. In the present systems, the lack of any significant π-bonding role for either sulphur ligand is confirmed, as is the greater basicity of thiolate than amine in CoN_2S_2 and of acetate over thiourea in

* Absolute absorbances have been estimated[11] for the CoN_2S_2 system so that the t parameter values in Table 3 can be scaled. All t values in the table for CoN_2S_2 are to be multiplied by 4.264×10^4 m^2 dm^3 mol^{-1} s^{-1}.

Table 3. Optimum energy (cm^{-1}) and intensity (arbitrary units) parameters for CoN_2S_2 and CoO_2S_2 chromophores

CoN_2S_2				CoO_2S_2			
e_σ(N)		3 900 (100)[a]		e_σ(O)		5 800 (200)	
				$e_{\pi\perp}$(O)		2 000 (200)	
e_σ(S)		5 800 (100)		e_σ(S)		2 600 (200)	
$e_{\pi\perp}$(S)		0 (100)		$e_{\sigma\perp}$(S)		−200 (200)	
B		620 (20)		B		690 (30)	
ζ		500[b]		ζ		500	
Σ		19 400[c]		Σ		20 400	
$^Pt_\sigma$(N)	30 (5)[d]	$^Ft_\sigma$(N)	0 (3)	$^Pt_\sigma$(O)	83 (5)	$^Ft_\sigma$(O)	100 (5)
				$^Pt_{\pi\perp}$(O)	50 (5)	$^Ft_{\pi\perp}$(O)	0 (5)
$^Pt_\sigma$(S)	100 (12)	$^Ft_\sigma$(S)	25 (3)	$^Pt_\sigma$(S)	4 (5)	$^Ft_\sigma$(S)	17 (5)
$^Pt_{\pi\perp}$(S)	0(5)	$^Ft_{\pi\perp}$(S)	0(3)	$^Pt_{\pi\perp}$(S)	0 (2)	$^Ft_{\pi\perp}$(S)	0 (2)

[a] Estimated errors in parentheses. [b] This parameter fixed throughout. [c] $\Sigma \equiv \sum_i^{\text{ligands}} (e_\sigma + e_{\pi\parallel} + e_{\pi\perp})_i$. [d] All t parameters relative to largest mean value = 100.

CoO_2S_2. At this stage, therefore, the intensity analyses serve to strengthen the conclusions of the energy analyses. It is on examination of the various $^Pt_\lambda$:$^Ft_\lambda$ ratios that the intensity analyses are seen to provide insight into the co-ordination beyond that from the traditional ligand-field energies alone. Discussion of the relative P and F contributions to transition moments is made in the light of the principles outlined in the Introduction. We refer in particular to the polarization of bonding electron density along the line of centres in a bond and to the lateral bulk of that density.

The greater P contributions for t_σ(N), t_σ(thiolate), and $t_{\pi\perp}$(O) all attest to short 'effective bond lengths' for these ligations: by this we mean the combination of actually short bonds with strong polarization of electron density towards the metal atom. In contrast, the relatively greater F contribution for t_σ(thiourea) accords with a longer bond and less ligand donation. All these features directly support the conclusions reached above. On the other hand, the close and strongly basic acetates in CoO_2S_2 are characterized with $^Pt_\sigma(O) < {}^Ft_\sigma(O)$, in marked contrast, for example, to the situation for the thiolate ligation in CoN_2S_2. In view of the smooth and unique nature of the intensity analysis and of the many correlations between energy and intensity analyses, both here and elsewhere,[7,9] we are disinclined to regard this feature merely as an artefact of the model or of imperfect analysis. Instead, we consider the larger F contribution associated with the Co–O σ bonding to characterize a 'thin' bond with compacted electron density. We imagine this to arise as part of a quite natural progression, as illustrated in Figure 6. On the left are sketched the changing electron distributions that one expected as ligands donate ever more negative charge to the metal. One discerns two features of these distributions: the electron density is polarized increasingly towards the metal, and the bond 'tightens' about the internuclear axis. The latter may be seen arising from an increased participation of core orbitals to the bonding orbital between more strongly interacting atoms, partly in order to minimize electron–nuclear separations. As discussed in the Introduction, while greater polarization of the bond orbital towards the metal favours P contributions to the local transition moment, compression into a 'thinner' bond favours F. On the right of Figure 6, therefore, we illustrate how these conflicting trends might be expected to accompany a smooth increase in ligand basicity. Thus we view the donation from the acetate ligands to be great enough to define a more compressed bond orbital than for the cobalt–thiolate interaction. In part, that must also be due to the smaller size of the donor atom. That the same trend is not observed for the π bonding in the cobalt–acetate link presumably attests to a lesser π compression towards the internuclear axis following greater shielding of the π cloud by the more compact, 'inner,' σ-electron density.

Conclusions

We refer to the calculation of both transition energies and intensity distributions as parts of the same c.l.f. model because they are predicated on the same underlying physical simplicity that Nature happens to bestow on transition-metal chemistry. Reasons for that simplicity and its consequences for our understanding of chemical bonding in this area have been discussed recently[4,17] at various levels of detail. The present view of '*d*–*d*' intensities as a property on a par with paramagnetic susceptibilities or e.s.r. g values demands that interpretations of the older ligand-field energy parameters and of the new intensity parameters should be made by simultaneous reference to the same chemical concepts. If these interpretations are to have chemical relevance we must employ the vocabulary of mainsteam chemical discussion. The, now large, experience we have of conventional ligand-field analysis has established confidence in pursual of the minutiae of any given study: we can support a closely focused view. We believe the much smaller number of intensity analyses completed thus far similarly encourage that same level of detailed enquiry.

So far we have addressed the intensities only of acentric chromophores, those which acquire their hues by virtue of the parity mixing that arises by static means. Shortly we shall report on analogous studies of centrosymmetric molecules where the intensity derives from dynamic processes. Meanwhile it is already clear that quantitative reproduction of the relative intensities of ligand-field '*d*–*d*' transitions is possible and apparently reliable. More interesting is the avenue this provides for mapping out more clearly than before the electron distributions in metal–ligand bonds.

Acknowledgements

We acknowledge the award of an S.E.R.C. research studentship (to M. J. D.).

References

1 M. Gerloch, J. H. Harding, and R. G. Woolley, *Struct. Bonding (Berlin)*, 1981, **46**, 1.
2 M. Gerloch and R. G. Woolley, *Prog. Inorg. Chem.*, 1984, **31**, 371.
3 M. Gerloch, 'Magnetism & Ligand-Field Analysis,' Cambridge University Press, 1983.
4 M. Gerloch, in 'Understanding Molecular Properties,' eds. J. S. Avery, J. P. Dahl, and A. Hansen, Reidel, Dordrect, Holland, 1987, p. 111.
5 M. Gerloch and R. C. Slade, 'Ligand-Field Parameters,' Cambridge University Press, 1973.
6 C. A. Brown, M. Gerloch, and R. F. McMeeking, *Mol. Phys.*, 1988, **64**, 771.
7 C. A. Brown, M. J. Duer, M. Gerloch, and R. F. McMeeking, *Mol. Phys.*, 1988, **64**, 793.
8 C. A. Brown, M. J. Duer, M. Gerloch, and R. F. McMeeking, *Mol. Phys.*, 1988, **64**, 825.
9 N. D. Fenton and M. Gerloch, *Inorg. Chem.*, 1989, **28**, 2975.
10 J. Mastrapaolo, J. A. Thich, J. A. Potenza, and H. J. Shugar, *J. Am. Chem. Soc.*, 1977, **99**, 424.
11 M. W. Makinen, S. C. Hill, M. Zeppezauer, C. L. Little, and J. K. Burdett, *J. Am. Chem. Soc.*, 1987, **109**, 4072.
12 A. R. Dale, M. J. Duer, M. Gerloch, and R. F. McMeeking, CAMMAG2, a FORTRAN program suite, 1987.
13 E. M. Holt, S. L. Holt, and K. J. Watson, *J. Am. Chem. Soc.*, 1970, **92**, 2721.
14 R. J. Deeth and M. Gerloch, *Inorg. Chem.*, 1985, **24**, 1754.
15 R. J. Deeth and M. Gerloch, *J. Chem. Soc., Dalton Trans.*, 1986, 1531.
16 N. D. Fenton and M. Gerloch, *Inorg. Chem.*, 1987, **26**, 3273.
17 M. Gerloch, *Coord. Chem. Rev.*, 1989, in the press.

Received 15*th August* 1988; *Paper* 8/03311K